Inelastic scattering of ^{6}Li from ^{58}Ni at 71 MeV

C. Williamson,* A. Galonsky, R. Huffman,† and R. Markham‡
Cyclotron Laboratory, Michigan State University, East Lansing, Michigan 48824
(Received 31 October 1979)

Nine excited states of ^{58}Ni were studied via the ^{58}Ni(^{6}Li,^{6}Li) reaction at 71.2 MeV. Two methods were employed to analyze the data. They were the distorted wave Born approximation, and the method of coupled channels. A comparison of their predictions and the information they provide about the nuclear deformation lengths is presented. In agreement with the Austern-Blair model for strongly absorbed particles, all five parameter sets produced equally good fits to the inelastic data.

[NUCLEAR REACTIONS ^{58}Ni(^{6}Li,^{6}Li') for ^{58}Ni* energies E^{*}=1.45, 2.46, 2.78, 3.04, 3.26, 3.62, 3.90, 4.48, and 4.75 MeV. Angular distributions measured, deformation lengths extracted.]

I. INTRODUCTION

Elastic[1-5] and inelastic [3,4] scattering of ^{6}Li by medium weight nuclei have been studied recently, but none of the studies has investigated inelastic transitions in ^{58}Ni with projectile energies above 34 MeV. In the present work nine inelastic transitions were observed in ^{58}Ni at 71 MeV. Each transition was treated as a one-phonon collective transition in the DWBA using complex coupling. Since the deformations of separate portions of the interaction potential (real, imaginary, Coulomb) need not necessarily be equal, the calculations were performed twice with each set of optical model (OM) parameters that fits the elastic scattering data.[5] These parameters are listed in Table I. In one set of calculations, the deformations were held equal, and in the other set of calculations the deformation lengths were held equal.

Preliminary coupled-channels calculations were also performed for the lowest energy, $0^{+}-2^{+}-4^{+}$, vibrational band which coupled the ground state and first two excited states. Investigations into multiple-plus-direct with admixtures of one-and two-phonon transitions for the first 4^{+} state at 2.45 MeV were performed with α-particle scattering as early as 1962 by Buck[6] and as recently as 1972 by Horen et al.[7] The studies were prompted by the fact that this state does not follow the Blair phase rule. According to this rule, angular distributions corresponding to even values of angular momentum transfer L should be out of phase with angular distributions corresponding to odd L transfer. Also, angular distributions with odd L should be in phase with the elastic distributions.

For the ^{90}Zr + ^{6}Li reaction at 34 MeV[3] and 75 MeV,[8] sizable differences have been noted between extracted deformation lengths and previously reported values. Surprise at these observations was one motivation in performing this investigation.

Table I. Optical model parameter sets which give the best fits to the elastic scattering data of Huffman et al.[5]

V	r_R	a_R	W	r_I	a_I
60	1.43	.84	17.6	1.78	.78
110	1.26	.86	18.0	1.77	.78
160	1.17	.87	18.8	1.76	.78
225	1.07	.89	19.9	1.74	.78
296	1.01	.89	21.5	1.72	.78

II. EXPERIMENTAL PROCEDURES

The MSU sector-focused cyclotron was used to produce an extracted beam of 200-300 nA of $^{6}Li^{+++}$ ions. An arc-like ion source[9] produced the beam through the sputtering action of Ne on LiF pellets, enriched in ^{6}Li. Electrodes of tantalum (source life, approximately three hours) were used, but hafnium was briefly employed in an attempt to increase source life.[10] (Hafnium did increase source lifetime by approximately a factor of two, but on-target current was reduced by a factor of approximately four.) Two analyzing magnets and several quadrupole focusing magnets were used to give a rectangular beam spot of approximately 2 mm x 4 mm on a foil target of 1.02 mg/cm^{2}, 99% enriched ^{58}Ni. On-target beam intensity of 10-50 nA at 71.2 MeV was monitored by stopping the beam in a Faraday cup and sending the current to an Ortec charge digitizer for charge measurements.

A detector with two resistive-wire, position-sensitive proportional counters in sequence backed by a scintillator, placed in the focal plane of an Enge split-pole spectrograph was used to gather the data. Two-dimensional gating techniques (ΔE vs TOF (time-of-flight), ΔE vs position, TOF vs position, and light vs position) were used for multiple identification of the scattered lithium ions. A PDP-11/45 on-line computer was used for gating, display, and collection of data.

The low beam intensity restricted the range over which it was possible to gather data to lab angles less than approximately 45°. A FWHM ~ 90 keV made it possible to resolve nine inelastic states. Typical spectra are displayed in Figure 1. For angles below 18°, the elastic peak was not recorded (see upper spectrum of Figure 1) in order to decrease dead-time in the detector. At the other angles, where the elastic peak was included in the spectra, we could obtain a check on the absolute values by comparison to the elastic-scattering data of Huffman et al.[5] at 74 MeV. To account for the 3-MeV difference, the OM parameter set (Table I) with V = 160 MeV was used to calculate the elastic scattering at 71 MeV. At some of the angles beyond 30°, where the runs were long, there were significant errors in our measurement of the elastic cross section. Therefore, we normalized our data by comparison of our elastic cross sections to those computed from

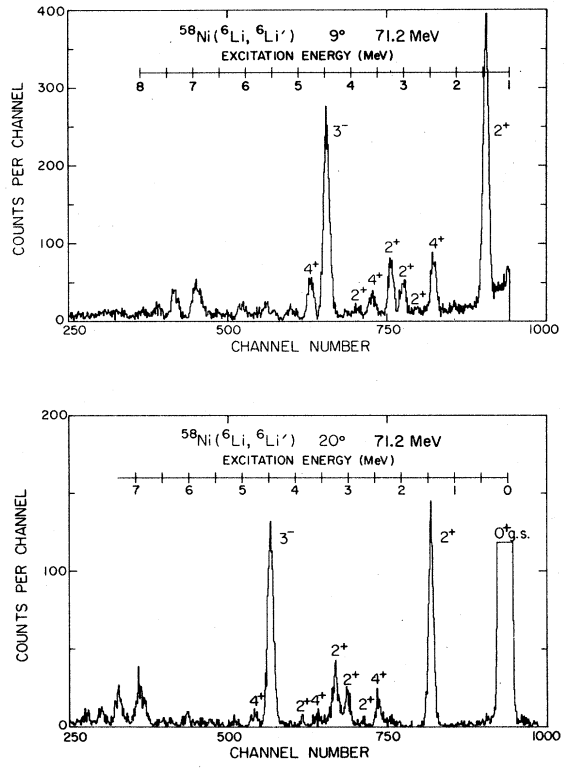

FIG. 1. Typical spectra.

Huffman's [5] data. The accuracy of the data, unless otherwise specified, is ± 5% relative with an additional ± 5% absolute.

III. DWBA ANALYSIS

Optical potentials with volume real and volume imaginary terms of the standard Woods-Saxon form were used in DWBA analysis of the data:

$$U(r) = -V f(r) - i W g(r),$$

where

$$f(r) = [\,1 + \exp(\frac{r-R_R}{a_R})\,]^{-1},$$

$$g(r) = [\,1 + \exp(\frac{r-R_I}{a_I})\,]^{-1},$$

and

$$R_R = r_R A^{1/3},\ R_I = r_I A^{1/3}.$$

Added to this was the potential due to a spherically symmetric, uniform charge distribution of radius R_c.

We used a first-derivative, collective-model form factor, with Coulomb excitation included, to describe the interaction:

$$F(r) = F_D(r) + F_c(r),$$

$$F_D(r) = -[V R_R \frac{df(r)}{dr} + i W R_I \frac{dg(r)}{dr}] \quad \text{and}$$

$$F_c(r) = \frac{3zz'e^2}{(2L+1)} \frac{R_c^L}{r^{(L+1)}}, \quad r > R_c,$$

$$= 0, \quad r < R_c,$$

where $R_c = 1.40\ A^{1/3}$ fm and hL is the angular momentum transferred. Coulomb excitation was significant mostly at small angles.

Calculations of the theoretical differential cross sections were performed on an XDS Σ–7 computer using the code DWUCK 72. [11] In the collective model,

$$(\frac{d\sigma_L}{d\Omega})_{Exp} = \beta_L^2 (\frac{d\sigma}{d\Omega})_{Th.}$$

Implicit in this model is the assumption that the deformation parameter β_L applies equally to the real, absorptive, and Coulomb terms in the potential, i.e. $\beta_{LR} = \beta_{LI} = \beta_{Lc}$. However, by appropriate scaling of V, W, and the Coulomb excitation scale factor, it is possible to set the deformation lengths $\delta_L = \beta_L R$ equal for each term in the interaction potential, i.e. $\beta_{LR} R_R = \beta_{LI} R_I = \beta_{Lc} R_c$. These two approaches to the DWBA analysis will henceforth be referred to as β scaling and β R scaling, respectively.

When discussing deformations measured by different experimental techniques, it is more common to compare deformation lengths $\delta_L = \beta_L R$. The nuclear matter deformation may then be obtained from the potential deformation through the relation $\beta_{LM} R_M = \beta_{LP} R_P$, where R_M, R_P, β_{LM}, and β_{LP} are the mass and potential radii and deformation parameters respectively. The choice of R_R, R_I, or R_c as R_P will be discussed in the next section.

Investigations were performed to facilitate a propitious choice for the matching radius and integration step size to be utilized in the distorted wave calculations. These investigations were performed on the elastic as well as the inelastic cross sections. In the latter case, angular distributions were obtained for integration step sizes between .035 and .30 fm for a matching radius of 14 fm and between .05 and .30 fm for a matching radius of 20 fm. As step size was decreased, the calculated differential cross sections for the two matching radii asymptotically approached the values obtained for a step size of 0.04 fm and 0.05 fm, respectively. These observations were based on an angular range of 0°-180°. However, it was found that in the angular range of our experiments, 5°-50°, the calculated angular distributions were quite similar for integration step sizes between 0.08 and 0.12 fm. Therefore an integration step size of 0.10 fm was used in subsequent analyses. Using this integration step size, angular distributions were then obtained for matching radii between 15 and 25 fm. When matching radii between 17 and 23 fm were used, the calculated angular distributions were nearly identical. Therefore, in subsequent analyses, we used 20 fm for the matching radius.

IV. DWBA RESULTS

The optical model parameter sets of Table I give the best fits to the elastic scattering of Huffman et al.[5] Results of the searches performed in fitting their data displayed signs of both continuous and discrete ambiguities. Each OM set of Table I corresponds to the best fit for each of the five "families" of parameters observed. It was hoped that our inelastic scattering data would remove or reduce the observed ambiguities when compared to DWBA inelastic angular distributions generated using these OM sets.

The theoretical inelastic angular distributions predicted by these five OM sets were very similar over the angular range for which data were obtained. In particular, the only observable differences were slight continuous changes in the depths of the minima with increasing value of the real potential depth V. These changes were most easily observable in the 2^+ states but did occur(to a much lesser extent) in the 3^- and 4^+ states. Also, these changes, even for the 2^+ states, were less than the

uncertainty in the data.

The above observations hold for both β and βR scaling; the difference between the two types of analyses being that βR scaling gives slightly deeper minima and a slightly steeper overall slope for all states. Also, there is little change in the quality of the fits to the data when switching from one type of analysis to the other for a particular set of OM parameters.

To illustrate the high degree of similarity between the theoretical angular distributions calculated using different OM sets, the extremes of these calculations are shown in Figures 2 and 3. In Figure 2 the V = 160 MeV fits to the data for β scaling (solid line) and βR scaling (dashed line) are shown together. Figure 3 shows the V = 60 MeV (solid line) and V = 295 MeV (dashed line) fits to the data when the β–scaling analysis technique is employed. Five of the states are fitted well by the DWBA but the predicted phase of the oscillations does not agree with the observed phase for the other four (viz. the 2.45 MeV (4^+), 2.78 MeV (2^+), 3.90 MeV (2^+), and 4.48 MeV (3^-) states). For the 2.45 MeV (4^+) state, this problem is given more consideration in the next section. Also, small-angle scattering

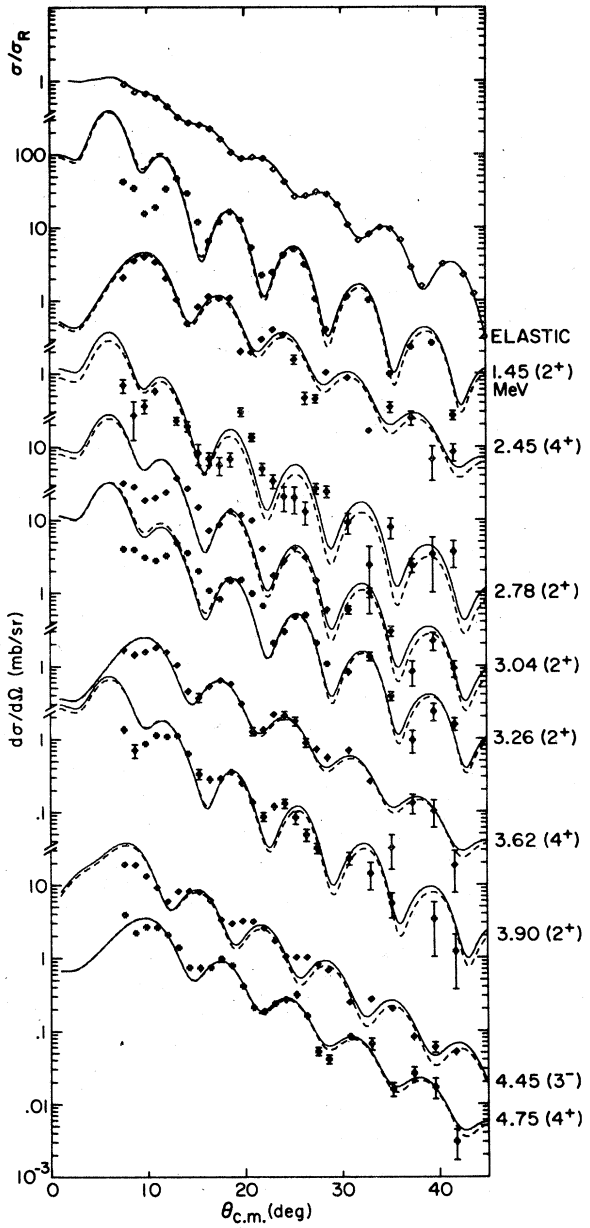

FIG. 2. Fits to the data for the V = 160 MeV optical model set using β scaling (solid line) and βR scaling (dashed line). Data for which error bars are not shown have uncertainties less than the size of the points. The elastic scattering data are from Huffman et al.[5]

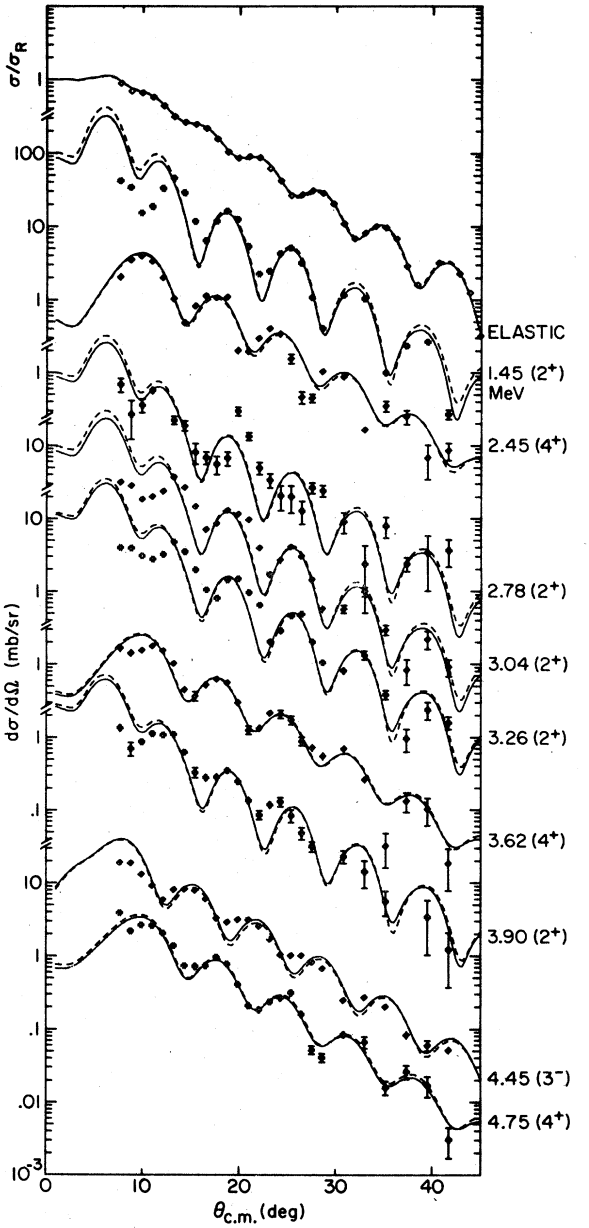

FIG. 3. Fits to data using V = 60 MeV (solid line) and V = 295 MeV (dashed line) optical model sets of Table I when using β scaling. Data for which error bars are not shown have uncertainties less than the size of the points. The elastic scattering data are from Huffman et al[5].

($\theta_{cm} \lesssim 15°$) is not well predicted for any of the 2^+ states.

Investigations were performed to find which element, if any, of the interaction potential (real, imaginary, Coulomb) was the major contributor to the cross sections. This information could lead to a proper choice of R_R, R_I, or R_c to be used as R_p in calculating the deformation lengths of the potential. Results showed that the imaginary term in the interaction potential gave contributions to the cross sections a factor of approximately three greater than the contributions due to the real term for each of the three angular momentum states observed. Also, Coulomb contributions to the cross sections were important only for the 2^+ states and then only for angles less than approximately 15°. Thus, R_I was chosen to be R_p and subsequently used to calculate the nuclear deformation lengths of the potential. The imaginary radius has also been used to calculate deformation lengths for other targets at different ^{6}Li beam energies.[3, 4]

In Table II, values of βR_I (from β scaling analysis technique) and βR (from βR scaling) are listed along with the δ values of previous analyses. The values of β, βR, and βR_I listed in Table II for this analysis were obtained by averaging the five values independently obtained from each OM set for a given state. The standard deviations associated with this averaging process are also listed in the table.

From Table II we see that the βR_I values are always about 20% greater than the βR values. In comparison to previous determinations of δ, βR_I is closer to δ_{AV} for five of the states and βR is closer for four of the states. Also, βR_I is within the range of previous determinations

Table II. Nuclear deformations and deformation lengths of this analysis with deformation lengths of previous analyses. The values reported for this analysis are averages of the values obtained independently from the five optical model sets of Table I. The numbers in parentheses after these values are the standard deviations in % associated with the averaging process. Previously reported values include the standard deviations in % and number of observations, respectively, in parentheses after their average. For (p,p'), (α,α'), and other reactions, δ is the average of values reported in Reference 12 and in References 13-16. δ_{AV} is the simple average of all values in the references incorporated in the six other columns of previously reported values. Methods of analysis used in extraction of δ_{AV} include DWBA, Austern-Blair diffraction model, coupled channels Born approximation, and measurement of electromagnetic transition strengths.

	β_L	βR_I	(β R)	δ_{AV}
	Present	Present		Previous
1.45 (2^+)	0.21(8)	1.41(7)	1.17(1)	.99(12,43)
2.46 (4^+)	0.054(4)	.37(4)	.31(2)	.51(14,4)
2.78 (2^+)	0.021(9)	.14(9)	.11(5)	.21
3.04 (2^+)	0.060(8)	.40(6)	.34(2)	.29(10,3)
3.26 (2^+)	0.066(7)	.45(5)	.38(4)	.35(12,4)
3.62 (4^+)	0.042(6)	.28(5)	.24(2)	.32(23,3)
3.90 (2^+)	0.032(6)	.22(5)	.18(1)	.18(9,2)
4.48 (3^-)	0.12(5)	.84(4)	.67(2)	.80(17,26)
4.75 (4^+)	0.050(6)	.34(5)	.29(2)	.44(18,3)

	δ(p,p')	δ(α,α')	δ(others)			
1.45 (2^+)	1.00(12,12)	.99(9,10)	(e,e') .90(13,2)	(d,d') .92(7,7)	(^{3}He,^{3}He') 1.01(8,4)	(^{16}O,^{16}O') 1.12(24,2)
			Coul. Ex. .87(12,10)	(n,n') 1.06	(^{18}O,^{18}O') 1.10(20,2)	
2.46 (4^+)	.56	.46(16,2)	(e,e') .57			
2.78 (2^+)		.21				
3.04 (2^+)		.28(13.2)	(e,e') .29			
3.26 (2^+)		.31(1,2)	(e,e') .40	(^{16}O,^{16}O') .37		
3.62 (4^+)	.39	.24 .33				
3.90 (2^+)	.19	.17				
4.48 (3^-)	.83(12,10)	.80(23,9)	(^{16}O,^{16}O') 1.00	(d,d') .66(4,2)	(^{3}He,^{3}He') .76(14,8)	
4.75 (4^+)	.53	.40(3,2)				

of δ for only two states, whereas βR is within the recorded range for five states. This is shown more clearly in Figure 4 where high, low, and average values of δ are shown with βR_I and βR.

In addition, the standard deviations associated with the βR_I are larger than those associated with βR by a factor of approximately three. Also noticeable for any given state is a trend in the individual values of βR_I (before averaging) to increase with increasing depth of the real potential when going from one OM set to another. No such trend was noticed in the βR values.

The βR values differ from the previously reported δ values most noticeably for the 4^+ states, but the difference is less than with β scaling. βR values for the other states do not agree well with the δ values either, except for the 2^+ states at 3.26 and 3.90 MeV. For the 4^+ states, the βR_I values agree with the δ values better than do the βR values, but the differences are still quite significant. Interestingly, note that βR_I and δ agree best (5% difference) for the 3^- state. Overall, though, the values of βR and βR_I of this analysis do not agree very well with the previously reported values.

Significant also is the fact that the ratios of $\beta_2 R_I / \beta_4 R_I$ (= 1.67) and $\beta_2 R / \beta_4 R$ (= 1.75) are quite similar and differ from the ratio of δ_2 / δ_4 (= 1.23) by about 40%. A similar observation may be made from recent analysis of lithium inelastic scattering from ^{90}Zr.[3] Thus, it would seem inaccurate to scale experimental lithium inelastic cross sections for all observed states by the amount required to obtain agreement with previously reported nuclear deformation lengths for 3^- states.

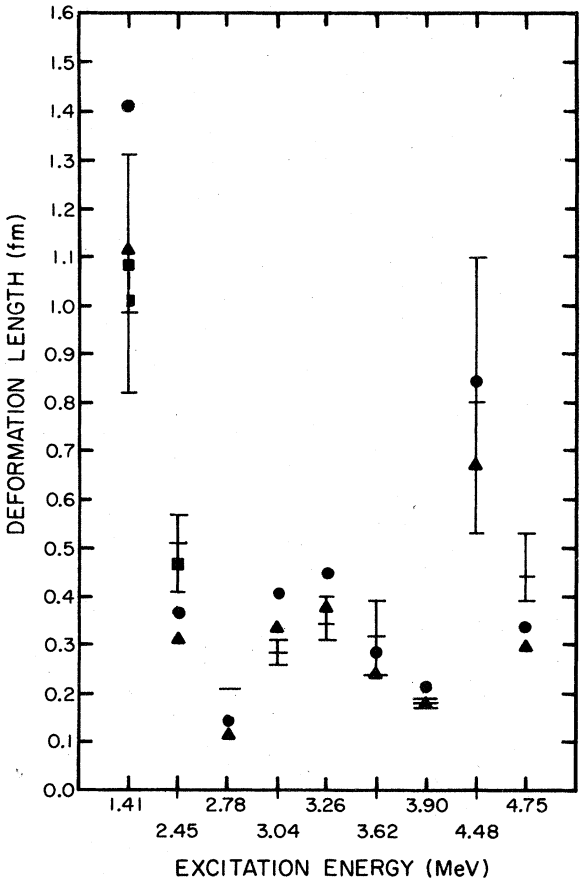

FIG. 4. Nuclear deformations of this analysis along with the ranges and averages of previous analyses - ● for βR_I (DWBA, β scaling), ▲ for βR (DWBA, βR scaling), and ■ for βR_I (coupled channels, first 2^+ and 4^+ only). See Table II for related values.

V. COUPLED CHANNELS ANALYSIS AND RESULTS

Coupled channels calculations were performed using the code ECIS.[17] The optical potential used was that of Table I with V = 160 MeV, and the computational parameters were set equal to those used in DWUCK 72: $R_{coul} = 1.40A^{1/3}$, 85 partial waves, and integration to a maximum radius of 20 fm in steps of 0.10 fm. The deformation parameters for each portion of the potential were set equal (i.e. $\beta_R = \beta_I = \beta_c$) and the transition matrix elements were calculated internally, in ECIS.

Only the ground state, 1.45 MeV (2^+), and 2.46 MeV (4^+) states were coupled in the present analysis. These states may be effectively coupled in the first-order vibrational model when the 4^+ state is assumed to be an admixture of one and two phonon components.[6,7,18] This allows for direct transitions to the 4^+ states, which are not usually included in first order. However, the second-order vibrational model was used because it was believed that reorientation matrix elements would have a sizable effect on the calculated angular distributions.[19] In fact, this effect was subsequently found to be negligible.

Initially, β_2 and β_4 were set to the values obtained from the previous DWUCK 72 analyses. The mixing parameter (BT) describing the mixing of one- and two-phonon components for the 4^+ state was initialized at 18.4° (10% 2 phonon and 90% 1 phonon). Searches were then performed on β_2, β_4, and BT, independently, forcing a simultaneous fit to the 2^+ and 4^+ states. Then a simultaneous search on all three was performed to optimize the fit (minimize χ^2) to the data. These results are given in Table III. It is seen that the coupling has decreased β_2 (from 0.21) and increased β_4 (from 0.054).

Results of the coupled-channels calcuations are shown in Figure 5. For elastic scattering, the differential cross sections for angles $\lesssim 25°$ were identical to those predicted by DWUCK 72, and for angles $\gtrsim 25°$, the differential cross sections were slightly lower and somewhat out of phase. This difficulty might be overcome by using the ECIS code to search on the OM parameters while fitting the elastic and inelastic scattering simultaneously. The fit to the 2^+ data was good except that the amplitude of the oscillations was too small. Therefore, the fit to the data was not quite as good as that predicted by DWUCK 72. The encouraging aspect of this analysis for the 2^+ state is that the small angle data ($\theta_{cm} \lesssim 15°$) were fitted much better than with DWUCK 72.

Finally, the fit to the 4^+ state was vastly improved.

Table III. Final values of the nuclear deformations, deformation lengths, and one- plus two-phonon mixing parameter, BT, obtained from coupled channels analysis.

	2^+	4^+
β_L	0.161	0.0686
$\beta_L R_I$	1.09	0.467
BT		43.75

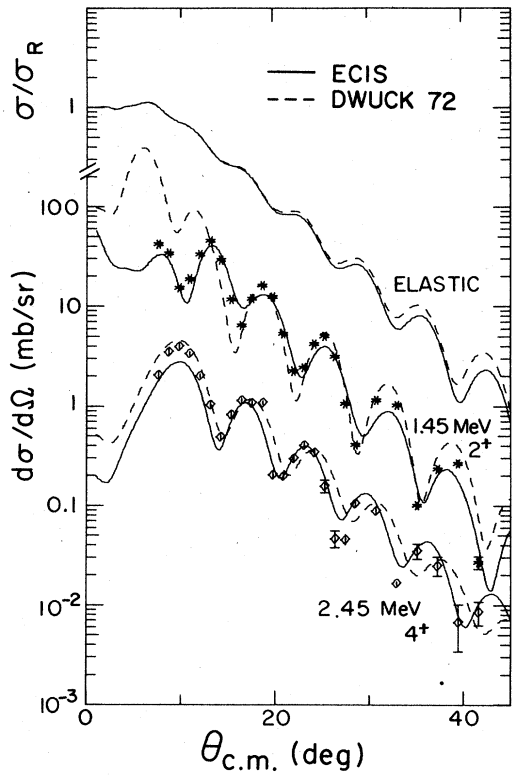

FIG. 5. Comparison of ECIS (solid line) and DWUCK 72 (dashed line) for elastic (ratio-to-Rutherford) and first two excited states.

The coupled channels analysis reproduced the phase of the data extremely well, and the amplitude of oscillation suggested a very good fit to the data. These were difficulties which the DWUCK 72 analysis could not overcome.

Listed with the final ECIS-related values of β_2, β_4 and BT in Table III are the calculated values of βR_I. The final value of BT represents a mixture of 53% 2 phonon and 47% 1 phonon coupling for the 4^+ state. The β_2 value from the coupled channels analysis does not agree with the previously reported value quite as well as that found with the DWUCK 72 analysis but the β_4 value from ECIS does agree better. Outstanding is the fact that the βR_I values determined here agree with previously reported values much better than do the values from either the β or βR scaling analysis techniques used in DWUCK 72. Also, both βR_I values are within the range of previous values.

Results of the present work confirm the observation of Buck [6] and of Horen et al. [7] that the 4^+ state at 2.45 MeV is an admixture of one- and two-phonon components. Buck investigated only the effects of multiple-plus-direct transitions and obtained good agreement with his 40-MeV alpha-scattering data when the direct two-phonon transition was enhanced by a factor of 1.5 over theoretical predictions. With the diffraction model of Austern and Blair, Horen et al. were unable to simultaneously fit the magnitude and slope of their alpha-scattering data at any of their experimental energies. However, they were able to reproduce the phase of the oscillations of their data. Coupled-channels calculations of the present work reproduced the magnitude, slope, and phase of our ^{6}Li data. Also, coupled-channels effects for the remaining 4^+ states of this analysis at 3.62 and 4.75 MeV appear to be much smaller because DWBA analyses reproduce these distributions well.

VI. CONCLUSIONS

No resolution or reduction of the OM ambiguities was possible through this DWBA analysis. Each of the five OM sets used to describe the interaction gave virtually identical fits to the elastic data over the angular range for which data were obtained and gave very similar fits to the inelastic data. The Austern-Blair model [20] for strongly-absorbed particles, such as ^{6}Li, predicts such behavior; i.e., that the elastic scattering determines the inelastic scattering. Hence, potentials producing the same elastic scattering will, in this model, produce the same inelastic scattering. A numerical study [21] involving Coulomb-nuclear interference has verified that results of the Austern-Blair model agree with those of a standard DWBA treatment. It is possible [22,23] that elastic data at more backward angles could remove the observed ambiguities.

Coupled-channels calculations were performed only as a preliminary study to explore their possible effect on inelastic states poorly fitted by the DWBA. It was found that these coupled-channels calculations were able to more accurately predict the phase of the oscillations for the 2.46 MeV (4^+) state and the cross sections at small angles for the 1.45 MeV (2^+) state. Finally, the deformation lengths obtained with the β values extracted from the coupled-channels calculations agreed with previously reported values better than did those produced by the DWUCK 72 calculations.

ACKNOWLEDGMENTS

This material is based upon work supported by the National Science Foundation under Grant No. Phy-78-22696. We gratefully acknowledge assistance in learning to use the code ECIS from R. Ronningen of this laboratory and from L. Foster of the University of Notre Dame.

*Present address: IBM Corporation, Rochester, Minn. 55901.
†Present address: Physics Dep't., University of Massachusetts, Amherst, Mass. 01002.
‡Present address: Xerox Corporation, Webster, N.Y. 14580.

[1] L.T. Chua, F.D. Becchetti, J. Janecke and F.L. Milder, Nucl. Phys. A273, 243 (1976).
[2] R.I. Cutler, M.J. Nadworny, and K.W. Kemper, Phys. Rev. C 15, 1318 (1977).
[3] R.J. Puigh and K.W. Kemper, Nucl. Phys. A313, 363 (1979).
[4] K.W. Kemper, A.F. Zeller, T.R. Ophel, D.F. Hebbard, A. Johnston, and D.E. Weisser, Nucl. Phys. A320, 413 (1979).
[5] R. Huffman, A. Galonsky, C. Williamson, and R. Markham, Michigan State University, to be published in Phys. Rev. C.
[6] B. Buck, Phys. Rev. 127, 940 (1962).
[7] Daniel J. Horen, J.R. Meriweather, B.G. Harvey, A.B. de Nercy, and J. Mahoney, Nucl. Phys. 72, 97 (1965).
[8] R. Pardo, R. Markham, W. Benenson, A. Galonsky, and E. Kashy, Phys. Lett. 71B, 301 (1977).

[9]E.D. Hudson and M.L. Mallory, Nucl. Sci. NS 23, 1065 (1976).
[10]P.S. Miller, H. Laumer, M.L. Mallory, and J.A. Nolen, Jr., IEEE Trans. Nuc. Sci. NS-26, No. 3, 3716 (1979).
[11]P.D. Kunz, University of Colorado, (unpublished).
[12]C. Michael Lederer and Virginia S. Shirley, Table of Isotopes, Seventh Edition, John Wiley & Sons, New York, 1978, pp 170-171.
[13]R.H. Bassel, G.R. Satchler, R.M. Drisko, and E. Rost, Phys. Rev. 128, 2693 (1962).
[14]H.W. Broek, J.L. Yntema, B. Buck, and G.R. Satchler, Nucl. Phys. 64, 259 (1965).
[15]G.R. Satchler, Nucl. Phys. 70, 177 (1965).
[16]S.A. Fulling and G.R. Satchler, Nucl. Phys. A111, 81 (1968).
[17]J. Raynal, Centre d'Etudes Nucleaires de Saclay, (unpublished).
[18]N. Lingappa and G.W. Greenlees, Phys. Rev. C 2, 1329 (1970).
[19]D.L. Hillis, E.E. Gross, D.C. Hensley, C.R. Bingham, F.T. Baker, and A. Scott, Phys. Rev. C 16, 1467 (1977).
[20]N. Austern and J.S. Blair, Ann. Phys. (N.Y.) 33, 15 (1965).
[21]C.K. Gelbke and J.G. Cramer, Phys. Rev. C 14, 1048 (1976).
[22]D.A. Goldberg, S.M. Smith, H.G. Pugh, P.G. Roos, and N.S. Wall, Phys. Rev. C 7, 1938 (1973).
[23]D.A. Goldberg and S.M. Smith, Phys. Rev. Lett. 29, 500 (1972).